Journal of Mathematical Chemistry Vol. 31, No. 4, May 2002 (© 2002)

Repro-modelling based generation of intrinsic low-dimensional manifolds

András Büki [a], Tamás Perger [a], Tamás Turányi [a] and Ulrich Maas [b]

[a] *Department of Physical Chemistry, Eötvös University (ELTE), H-1518 Budapest, P.O. Box 32, Hungary*
E-mail: turanyi@garfield.chem.elte.hu
[b] *Institut für Technische Verbrennung, Universität Stuttgart, D-70550 Stuttgart, Germany*

Received 16 May 2002

Effective procedures for the reduction of reaction mechanisms, including the intrinsic low-dimensional manifold (ILDM) and the repro-modelling methods, are all based on the existence of very different time scales in chemical kinetic systems. These two methods are reviewed and the advantages and drawbacks of them are discussed. An algorithm is presented for the repro-modelling based generation of ILDMs. This algorithm produces an unstructured table of ILDM points, which are then fitted using spline functions. These splines contain kinetic information on the behaviour of the chemical system. Combustion of hydrogen in air is used as illustrative example. Simulation results using the fitted model are compared with the outcome of calculations based on the detailed reaction mechanism for homogeneous explosions and 1D laminar flames.

KEY WORDS: chemical kinetics, mechanism reduction, time scale analysis, slow manifolds

1. Introduction

As a result of the astonishing progress of reaction kinetics in the last decades, detailed reaction mechanisms are available for many chemical processes (see, e.g., [1,2] for references). New mechanisms for methane combustion and for NO_x production in flames are presented and tested in two recent papers [3,4]. These papers contain several references to other recent mechanisms in these two fields. The detailed mechanisms frequently well reproduce the experimental data, but simulations based on them are too slow when these mechanisms are used for the simulation of spatially inhomogeneous systems, like turbulent flames or atmospheric chemical systems. Several methods have been proposed for the reduction of reaction mechanisms [5]. Reduction of a mechanism means the generation of a chemical or mathematical model that provides a practically identical solution to the original detailed mechanism for a subset of conditions. Mechanism reduction methods can eliminate redundant species and reactions from the mechanism, but the most successful methods, in terms of computer time saving, are all based on the time scale separation in chemical kinetic systems. This time scale separation allows decoupling various parts of the original system in such a way that the slower subsystems

0259-9791/02/0500-0345/0

determine the long time behaviour of the faster subsystems. Of the several methods based on time scale separation, two methods, the repro-modelling and the ILDM, are reviewed here. A combination of the two methods is presented and features of the new algorithm are studied using the example of hydrogen–air combustion.

2. Repro-modelling and ILDM

2.1. Repro-modelling

The idea of repro-modelling emerged from the observation that complex computational models frequently include very time-consuming submodels [6]. If information is exchanged between the main model and the submodel via a few variables only, then it is possible to "map" the behaviour of the submodel and to replace it by simple algebraic functions. Generation of the algebraic functions can be based on initial value sensitivities [7] or probing the submodel with many possible inputs and fitting the output of the model as a function of input data [8,9]. The detailed model can be, for example, a computational fluid dynamic (CFD) code that calculates concentration changes in a spatially inhomogeneous system due to chemical reactions, diffusion and convection. In most CFD codes the effect of chemical reactions is computed by a "chemical kinetics" box. This module can be replaced by fitted functions if the following algorithm is used:

(i) Several hundred or thousand spatially homogeneous chemical kinetic simulations are carried out using a detailed reaction mechanism. The conditions and parameters of the simulations are selected in such a way that they cover the regions of the subsequent CFD calculations. Results of the calculations are recorded in a database.

(ii) Points in the database are fitted with simple algebraic functions (e.g., polynomials). The requirement is fitting several ten thousand data points within an accuracy of about 1%.

(iii) During the CFD calculations these algebraic functions are used for the evaluation of the chemical source terms.

In this case, input variables of the repro-model can be the actual local concentrations and the varying parameters (like temperature or, in case of photochemical reactions, light intensity). Depending on the complex model, the output can be concentrations, production rates of species or change of concentrations during a predefined time step Δt. In the latter case the integrated solution is fitted which means that time integration of chemical kinetic equations is avoided during the run of the complex CFD model.

Calculation of the submodel via fitted functions can be up to 10^4 times faster [10]. It is not unusual that calculation of chemical changes consume 99% of computer time in a CFD model, therefore simulation of the model can be about 100 times faster, if chemical changes are calculated by the repro-model. Also, properly selecting the fitting function, any accuracy of the reproduction of the detailed model can be achieved.

Repro-modelling has been used in many fields (maybe under different names) where dynamical systems with very different time-scales are simulated. In chemistry, repro-modelling has been applied in atmospheric chemistry [7,8,11–13], for the simulation of the Belousov–Zhabotinsky oscillating reaction [9], CO ignition [10], spread of shock waves in H_2/O_2 mixtures [14] and low temperature hydrocarbon oxidation [15]. In a recent application of repro-modelling [12], fitted model of 9 variables was used to describe photo-oxidant generation in the troposphere.

A unique advantage of the repro-modelling method is that simulation results, not directly related to the local behaviour in the variable (concentration) space, can also be fitted and predicted. For example, in an industrial safety problem the output of the chemical kinetics box can be the time-to-ignition of a fuel–air mixture.

2.2. Intrinsic low-dimensional manifolds

An apparently entirely different approach for mechanism reduction is based on the existence of intrinsic low-dimensional manifolds (ILDMs) in the composition space [16]. The dimension of the composition space in a combustion system corresponds to the number of species. It is about 40 for methane oxidation and typically around 2000 for the low-temperature oxidation of higher hydrocarbons. The real dynamic dimension after a short initial phase is much less because trajectories quickly relax towards slow manifolds in the composition space.

The dynamic dimension, needed to describe the essential features, was found to be 2 or 3 in case of many combustion systems. This means that the state vector can be given (in a tabulated or fitted form) as a function of 2 or 3 variables. Having the system relaxed to low dynamic dimension, the dynamic information of the system is completely characterised by knowing the location of the ILDM in the composition space and the direction and rate of change of the system on the manifold. This information can be calculated numerically at any point of the manifold by using the equations below.

Let the chemical system be described by the system of ordinary differential equations

$$\frac{\mathrm{d}\boldsymbol{\psi}}{\mathrm{d}t} = \mathbf{f}(\boldsymbol{\psi}), \tag{1}$$

where $\boldsymbol{\psi} = (h, p, y_1, y_2, \ldots, y_n)^{\mathrm{T}}$. Here h is the enthalpy, p is the pressure, $\mathbf{y}$ is the vector of specific mole numbers, defined as $y_i = w_i/M_i$, where w_i is the mass fraction of species i and M_i is the molar mass of species i.

Now let the Jacobian of the ODEs be decomposed into a slow and a fast subspace:

$$\mathbf{J} = \frac{\partial \mathbf{f}}{\partial \boldsymbol{\psi}} = (\mathbf{Z}_{\mathrm{s}}\ \mathbf{Z}_{\mathrm{f}}) \begin{pmatrix} \mathbf{N}_{\mathrm{s}} & 0 \\ 0 & \mathbf{N}_{\mathrm{f}} \end{pmatrix} \begin{pmatrix} \hat{\mathbf{Z}}_{\mathrm{s}} \\ \hat{\mathbf{Z}}_{\mathrm{f}} \end{pmatrix}, \tag{2}$$

where

$$(\mathbf{Z}_{\mathrm{s}}\ \mathbf{Z}_{\mathrm{f}}) \begin{pmatrix} \hat{\mathbf{Z}}_{\mathrm{s}} \\ \hat{\mathbf{Z}}_{\mathrm{f}} \end{pmatrix} = \mathbf{I} \tag{3}$$

and the eigenvalues of $\mathbf{N}_\mathrm{s}$ are given by $\lambda_1, \lambda_2, \ldots, \lambda_m$, the eigenvalues of $\mathbf{N}_\mathrm{f}$ are given by $\lambda_{m+1}, \ldots, \lambda_n$, and $\lambda_i^{\mathrm{real}} \geqslant \lambda_j^{\mathrm{real}}$ for $i < j$. In this way $\hat{\mathbf{Z}}_\mathrm{f}$ forms an invariant left subspace associated with the smallest eigenvalues. In the following assume that the splitting has been performed such that $\lambda_m^{\mathrm{real}} \neq \lambda_{m+1}^{\mathrm{real}}$ and $\lambda_{m+1}^{\mathrm{real}} < 0$.

The ILDM is defined in such a way that there is no movement in the fast directions and therefore the product of matrix $\hat{\mathbf{Z}}_\mathrm{f}$, which contains the fast directions, and vector $\mathbf{f}$, which defines the direction of the actual movement of the system, is zero.

$$M_m = \left\{ \boldsymbol{\psi} \mid \hat{\mathbf{Z}}_\mathrm{f}(\boldsymbol{\psi})\mathbf{f}(\boldsymbol{\psi}) = 0 \right\}. \tag{4}$$

This equation can be solved by various methods [16,17], and an efficient multidimensional continuation procedure has been reported in [18].

Advantages of the ILDM approach are that a reduced model having the minimal applicable dynamical dimension can be produced, that the procedure above can be automated, and that there is no need for making *a priory* QSSA or partially equilibrium approximations. A disadvantage is the complexity of the computational algorithm.

A possible objection against the ILDM method is that it might not be applicable if the dimension of the manifold is not low enough (simply due to storage requirements). Tabulated manifolds have been generated up to a manifold dimension of 5 [19]. However, if one makes use of the fact that the accessed domain covers only a small subdomain of the state space (see [20] or [21]), and that the dimension can be adapted locally (increase dimension only where necessary), higher dimensions are feasible to attain.

2.3. Combined repro-modelling and ILDM approaches

In one version of the repro-modelling approach, the variables of the fitted function are identical to the variables of the submodel. In this case, the repro-modelling approach allows fitting the solution of the ODE by storing the change of variables during a predefined time step Δt. This means that, at the application of such a model, the time-consuming solution of stiff ODEs are replaced by simple evaluation of polynomials and therefore computer time is saved [9], although the number of variables is still the same. Further savings can be achieved without significant loss of accuracy if the number of variables of the repro-model is selected to be identical to the dynamic dimension of the submodel [10], which is smaller than the overall dimension of the system. In this case, homogeneous simulations are carried out using the original detailed model, but the input–output relations are recorded only after some initial time, when the trajectories of simulations have approached the appropriate manifold, and the results of simulations can be represented by a few variables only. This will yield good results only if the dimension of the fitting variable space is at least equal to the dimension of the attracting manifold. Therefore, probing the dataset by a series of fitting functions having gradually decreasing number of variables can be used to assess the dimension of the low-dimensional attractors. The accuracy of fitting is suddenly deteriorated [10] when the number of variables is not enough to represent the data. This method, although it works well in some cases, is laborious and may include pitfalls. Thus, a key improvement of

the repro-modelling approach can be made if a direct monitoring of the dimension of the collected data is performed. This will be discussed in the next section. The proposed new method represents an alternative way to the generation of ILDMs and inherits some good features from both the repro-modelling and ILDM approaches.

3. Repromodelling based ILDM generation – a general algorithm

The m-dimensional ILDM contains the points in the state space where the fastest time scales have been relaxed. The calculation of the ILDM, though possible (see, e.g., [16,18]) is rather difficult from a numerical point of view. Furthermore, three important things are worthwhile to note:

(i) For most calculations, the ILDM does not have to be known to an extremely high accuracy, but it is sufficient to know a small domain Ω_m^M that describes the neighbourhood of the ILDM.

(ii) In typical applications it is not necessary to know the whole domain of existence of the ILDM because large parts of the ILDM are never accessed in practical applications (see, e.g., [20]).

(iii) If the ILDM is represented by a fitted function and not by a look-up-table in the simulation code, the method for its generation does not have to be based on a structured grid.

These observations lead to a new way of identifying and storing the ILDMs. It is based on three ingredients:

(i) The determination of set ${}^p\Omega_m^M$ of p points in state space, which are close to the manifold in a sense to be described later.

(ii) Calculation of the properties of the state under the condition that the fastest time scales have already relaxed, e.g., the rates of the slow chemical processes, information on the back-relaxation of perturbations towards the manifold.

(iii) Approximation of the set ${}^p\Omega_m^M$ by an m-variable fitting function.

Let us assume that the dynamical behaviour of a complex system shall be approximated by an m-dimensional manifold. Of course, a generalisation to an adaptive dimension depending on the domain in the state space is possible, but shall not be considered here. The manifold M_m can be calculated using equation (4). However, in most cases it is not necessary to know the manifold exactly, but only with a given accuracy, which depends on the desired accuracy of the representation. This means that the manifold M_m is approximated by domain $\Omega_m^M = \{\boldsymbol{\psi} \mid \delta(\boldsymbol{\psi}, M_m) < \varepsilon\}$, where δ is a suitable measure for the distance of a point from the manifold, to be specified below. Domain Ω_m^M is a subset of the n-dimensional state space that is in the neighbourhood of the m-dimensional manifold M_m. As the trajectories of the chemical kinetics simulation approach the manifold M_m, the distance decreases until it is zero at the equilibrium value.

There are different ways of determining how close the trajectory is to an m-dimensional manifold. One is based on the determination how far the state $\boldsymbol{\psi}(t)$ is away from state $\boldsymbol{\psi}^m(\boldsymbol{\psi}(t))$, where $\boldsymbol{\psi}^m(\boldsymbol{\psi}(t))$ is the state which is obtained starting from $\boldsymbol{\psi}(t)$ and assuming that the system evolves with the slow modes frozen:

$$\boldsymbol{\psi}^m\big(\boldsymbol{\psi}(t)\big) = \boldsymbol{\psi}(\tau \to \infty), \tag{5}$$

where

$$\frac{\mathrm{d}\boldsymbol{\psi}}{\mathrm{d}t} = \mathbf{Z}_\mathrm{f}(\boldsymbol{\psi})\hat{\mathbf{Z}}_\mathrm{f}(\boldsymbol{\psi})\mathbf{f}(\boldsymbol{\psi}), \quad \boldsymbol{\psi}(\tau = 0) = \boldsymbol{\psi}(t). \tag{6}$$

In this case point $\boldsymbol{\psi}(t)$ can be assumed to be close to the manifold if $\|\boldsymbol{\psi}(t) - \boldsymbol{\psi}^m(\boldsymbol{\psi}(t))\| < \varepsilon$. Accordingly, the distance can be defined as $\delta = \|\boldsymbol{\psi}(t) - \boldsymbol{\psi}^m(\boldsymbol{\psi}(t))\|$. This methodology can be found, e.g., in [22,23].

A simpler method can be derived if one makes use of the fact that the trajectories approach the ILDM sooner or later. Thus, one can monitor the evolution of trajectory $\boldsymbol{\psi}(t)$. Let us assume that we are at a given point $\boldsymbol{\psi}^0$ in the state space and want to find the corresponding point on the manifold, which fulfils equation (4). Then the first step of a Newton iteration is given by:

$$\hat{\mathbf{Z}}_\mathrm{f}\big\{\mathbf{f}(\boldsymbol{\psi}^0) + \mathbf{J}\big({}^1\boldsymbol{\psi}^m - \boldsymbol{\psi}^0\big)\big\} = 0, \tag{7}$$

$$\hat{\mathbf{Z}}_\mathrm{s}\big({}^1\boldsymbol{\psi}^m - \boldsymbol{\psi}^0\big) = 0 \tag{8}$$

leading to

$$\hat{\mathbf{Z}}_\mathrm{f}\big({}^1\boldsymbol{\psi}^m - \boldsymbol{\psi}^0\big) = -\mathbf{N}_\mathrm{f}^{-1}\hat{\mathbf{Z}}_\mathrm{f}\mathbf{f}\big(\boldsymbol{\psi}^0\big), \tag{9}$$

$$\hat{\mathbf{Z}}_\mathrm{s}\big({}^1\boldsymbol{\psi}^m - \boldsymbol{\psi}^0\big) = 0. \tag{10}$$

Thus, an evaluation of $-\mathbf{N}_\mathrm{f}^{-1}\hat{\mathbf{Z}}_\mathrm{f}\mathbf{f}(\boldsymbol{\psi}(t))$ allows an estimate of the first Newton correction, and if

$$\big\|{}^1\boldsymbol{\psi}^m - \boldsymbol{\psi}^0\big\| = \big\|-\mathbf{Z}_\mathrm{f}\mathbf{N}_\mathrm{f}^{-1}\hat{\mathbf{Z}}_\mathrm{f}\mathbf{f}\big(\boldsymbol{\psi}(t)\big)\big\| < \varepsilon, \tag{11}$$

then state $\boldsymbol{\psi}(t)$ can be assumed to be sufficiently close to the manifold. Here a suitable choice for the error tolerance ε depends on the definition of the norm. If a submultiplicative matrix norm is chosen, we obtain

$$\big\|{}^1\boldsymbol{\psi}^m - \boldsymbol{\psi}^0\big\| = \big\|-\mathbf{Z}_\mathrm{f}\mathbf{N}_\mathrm{f}^{-1}\hat{\mathbf{Z}}_\mathrm{f}\mathbf{f}\big(\boldsymbol{\psi}(t)\big)\big\| \leqslant \|\mathbf{Z}_\mathrm{f}\| \cdot \big\|-\mathbf{N}_\mathrm{f}^{-1}\hat{\mathbf{Z}}_\mathrm{f}\mathbf{f}\big(\boldsymbol{\psi}(t)\big)\big\|. \tag{12}$$

If we also perform an eigenvector decomposition, we can use the condition $|\hat{\boldsymbol{v}}_i\mathbf{f}(\boldsymbol{\psi}(t))/\lambda_i| < \varepsilon_i$ to guarantee that the state is sufficiently close to the manifold. In this case $\mathbf{N}_\mathrm{f}$ is a diagonal matrix, vector $\hat{\boldsymbol{v}}_i$ denotes the ith row of matrix $\hat{\mathbf{Z}}_\mathrm{f}$ and the eigenvectors can be normalised such that $\|\hat{\boldsymbol{v}}_j\| = 1$. A different theoretical derivation of the latter condition has been discussed by Tomlin et al. [24]. An alternative algorithm for the determination of the dimension of long-time dynamics was recently published by Handrock-Meyer et al. [25]. In this paper conditions are given to guarantee that the splitting of the eigenvalue spectrum of the Jacobian implies a separation of the corresponding transformed variables into fast and slows categories.

The method described above allows determining whether point $\boldsymbol{\psi}$ belongs to the domain Ω_m^M, which describes the neighbourhood of the ILDM. Now let us turn to the question of how a set of points can be generated such that all states accessed in an application lie in the domain Ω_m^M. We look for set ${}^p\Omega_m^M$ of p points, which are spread over the whole domain Ω_m^M in such a way that they cover the part of the manifold which is accessed in an application, and which are sufficiently close to each other in order to allow an accurate representation. In general, application of the repro-modelling methodology offers a way for the generation of such points, because making the repro-model the aim is to generate a set of results (outputs) that is representative to the submodel at the conditions of planned applications. The exact ways of obtaining such points differ from one physical system to another. In combustion simulations, a usual task is making reduced mechanisms applicable for flame simulations. In the next section, an algorithm will be provided, which is based on selecting the initial conditions of the homogeneous reactor calculations by mixing burnt and fresh mixtures. Other possibilities would be to start the simulations from results of laminar or turbulent flame calculations or simply to pick initial points at random in the reaction space. The latter is a general approach, but the conditions for the resulting manifold points have to be checked during the procedure. These points have to cover the part of the manifold that is accessed in the application, and have to be close enough to allow an accurate representation.

The accuracy of the reduced model obtained depends on the errors introduced during the creation of the model. It inherits the errors introduced by the application of slow manifolds. A quantitative study associated with the errors of the ILDM method for different dimensions has been carried out by Schmidt and Maas [22]. An other source of errors is associated with the fitting procedure. However, the error of fitting can be controlled directly by calculating the local deviation between the database points and the fitted functions.

To summarise, the overall algorithm can be written as follows:

DO
- Generate an appropriate initial value $\boldsymbol{\psi}_0^i$;
- Start from this initial value and calculate trajectory $\boldsymbol{\psi}(t)$ for $t \to \infty$;
- Monitor the states $\boldsymbol{\psi}(t)$ during the solution and determine whether $\boldsymbol{\psi}(t)$ is in the neighbourhood of the manifold using equation (5) or (12).
- If $\boldsymbol{\psi}(t)$ is in Ω_m^M, store $\boldsymbol{\psi}(t)$ and all necessary information, e.g., the reaction rates $\mathbf{f}^m = \mathbf{Z}_s(\boldsymbol{\psi})\hat{\mathbf{Z}}_s(\boldsymbol{\psi})\mathbf{f}(\boldsymbol{\psi})$ assuming that the slow modes are completely exhausted.
- Leave the loop
  - if enough points have been found to cover all the accessed space, which can be monitored by checking convexity conditions (see, e.g., [20]) and
  - if the collected points allow an accurate representation of the manifold, which can be monitored by a condition for the maximum distance between the points or by interpolation error analysis.

ENDDO

Approximate domain Ω_m^M by m-variate functions (e.g., multivariate splines, orthogonal polynomials) or by unstructured grids with multilinear interpolation.

This formal algorithm will be explained in the following section using the example of a hydrogen–air combustion system.

4. Manifold for H_2/air flames

4.1. Generation of unstructured ILDM tables

Oxidation of hydrogen in air at atmospheric pressure is one of the best-known combustion processes. The Leeds methane oxidation mechanism [3] includes a complete and detailed hydrogen oxidation mechanism, which is also available from the Leeds Mechanism web sites [26]. This hydrogen oxidation mechanism has been tested [3] against flame velocity and shock tube data and good agreement is found. This detailed mechanism is used in our calculations.

Combustion of hydrogen can be described with reasonable accuracy for many problems by a single reaction progress variable [27], if the fuel-to-air ratio and the enthalpy are fixed. If we allow varying the fuel-to-air ratio, but assume equal diffusivities and Lewis number of one (for nonunity Lewis number see [28]), the combustion of hydrogen can be described by a 2D ILDM, where one dimension stems from the chemical kinetics and one from the varying conserved quantities. Since the manifold is attractive, trajectories of all homogeneous simulations will approach the manifold after some time. The manifold is characterised by the H : O : N ratio and enthalpy which correspond to the gas mixture at the cold boundary of the premixed flame. The strategy for the generation of such 2D ILDMs for H_2/air flame simulations must follow the requirements specified in the last section, that we need a set of points which approximate the 2-dimensional manifold in the domain of interest in the composition space. There are various possible choices. Here we present a very simple and straightforward one, which is based on homogeneous reactor calculations for varying element compositions.

First, only composition C of the unburnt mixture is known and a standard procedure, outlined in the caption of figure 1, is used to find the corresponding equilibrium point. The high temperature equilibrium state is denoted by letter E in figure 1. Then cold gases with composition C and the equilibrium composition E are mixed using different mixing ratios (dots 3 in the figure) stepping towards state C. For each mixture an adiabatic homogeneous reactor calculation is performed to check if the mixture is combustible. The last, still combustible mixture composition is used as a starting point of an adiabatic homogeneous calculation, which is allowed to run to the equilibrium point (curve 4). During this calculation, eigenvalues and eigenvectors of the Jacobian are calculated at each step of the ODE solver, and actual dimension of the points are continuously evaluated. Concentration values are recorded when the dimension analysis indicate that the points are close to a 1D manifold in reaction space, corresponding to

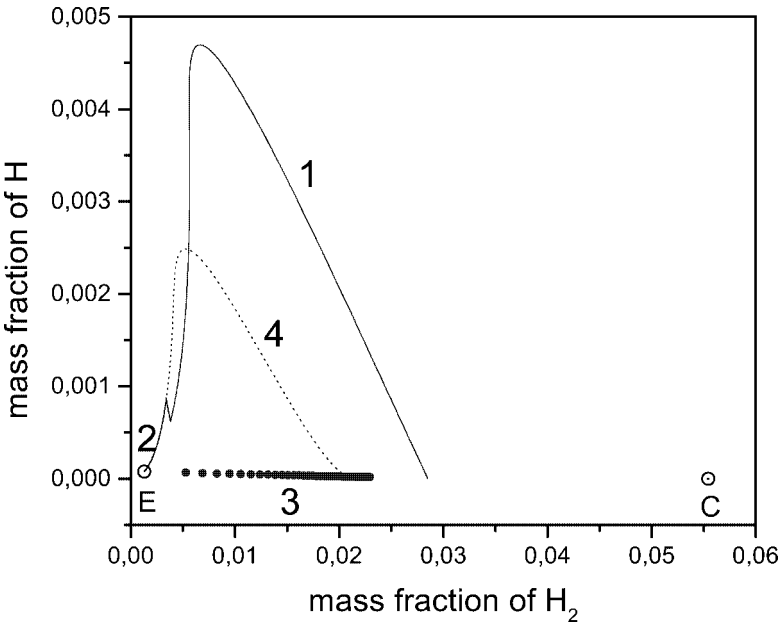

Figure 1. Graphical characterisation of the algorithm for the repro-modelling based generation of ILDMs for premixed hydrogen–air flames. Point C: the cold mixture; point E: point of equilibrium (burnt state). Point E was determined by raising the temperature of the cold mixture above the ignition limit. Curve 1 shows the trajectory of the system after ignition. Then, enthalpy of the mixture was set to back to the level of the cold mixture and the calculated trajectory (curve 2) ended up in point E. Combustible limit was found by mixing compositions C and E in several steps (dots 3). Trajectory from the just combustible state to point E is denoted by number 4. The points of the trajectory that belong to the manifold are recorded in the database.

one reaction progress variable (note that the overall dimension of the ILDM will be 2, because the analysis is repeated for varying fuel to air ratios). The dimension analysis is based on counting the conserved, active, and relaxed modes using an eigenvector–eigenvalue decomposition of the Jacobian. The number of conservation relations n_{c} is known *a priori*, because it is equal to the number of elements. In accordance with equation (12), a point is considered to be relaxed to direction i if $|\hat{\mathbf{v}}_i \mathbf{f}/\lambda_i| < c_{\mathrm{r}}$, where c_{r} is an appropriate small threshold value, which was chosen to be $c_{\mathrm{r}} = 1$ here. The estimated dimension of the trajectory is equal to $n_{\mathrm{D}} = n - n_{\mathrm{c}} - n_{\mathrm{r}}$, where n is the number of variables and n_{r} is the number of relaxed modes.

Combustion of hydrogen for a given cold boundary composition, pressure, and enthalpy can be described by a one-dimensional ILDM. Varying the cold mixture composition and the enthalpy, the appropriate several-dimension manifolds for hydrogen combustion can easily be generated. In our calculations a single enthalpy value of $h = 0$ J was considered, which corresponds to hydrogen–air flames with 298 K cold boundaries. The fuel-to-air ratio was varied from $\varphi = 0.5$ to $\varphi = 6.0$ in steps of $\varphi = 0.1$ and the above procedure was repeated for each φ value. Selection of this fuel-to-air ratio range can be justified by premixed hydrogen–air flame simulations [3], which indicated

that the flame velocity was very small and the mixtures were hardly combustible outside these φ values. This means that the fitted mechanism is expected to work in a wide range of premixed flame conditions. Also, it is applicable in diffusion flame calculations, because outside this φ range mixing and diffusion have a much higher influence on the concentration changes than chemical reactions.

As shown above, generation of two-dimensional ILDMs for the hydrogen–oxygen system is quite simple. ILDMs of higher dimensions can also be calculated using the combined repro-modelling–ILDM approach. One possibility is to generate additional initial values for homogeneous reactor calculations by randomly mixing several chemical states in the composition space. Another possibility is to start from results of laminar flame calculations. In any case, it has to be guaranteed only that the points in state space span the whole range of compositions of interest and that the points obtained from the procedure are able to approximate the manifold with a desired accuracy. A third possibility would be to perform the analysis during a CFD-calculation, i.e., to perform an *in situ* tabulation similar to the ISAT technique developed by Pope [29].

4.2. Fitting the ILDM database

The strategy described above yields a large number of points, which approximate the manifold. For the hydrogen–air example the algorithm generated a database of 79526 points. The collected data all lay on a 2D manifold as can be seen in figure 2. Points, very close to each other, do not carry new information and therefore points that belong to the same φ and have a temperature difference less then 1K were deleted. This step decreased the number of points to 25708. The database used in this work contained for each point the values of the mass fractions, temperature, and time derivative of the mass fraction of H_2O (i.e., production rate of water). If the repro-model provides the production rate of water, then the reaction progress can be obtained by integrating the corresponding single variable differential equation. An alternative method is to store the change of water mass fraction during a predefined time step. In this way the integrated solution is fitted and therefore, during the flame calculation, integration is replaced by the calculation of the concentration set belonging to time Δt later, which is computationally very efficient [10]. This approach is similar to the storage of integrated solutions in the look-up tables that are used in turbulent flame calculations. In the example considered here, calculations indicated that time steps $\Delta t = 10^{-4}$ s and 10^{-5} s could be used successfully and therefore change of water mass fraction during these time steps were also added to the database. Mass fraction of N_2 and H_2O were selected as a representative of local fuel-to-air ratio and reaction progress variable, respectively. Selection of these two independent variables allows a unique representation of the manifolds, because the concentration of water is continuously increasing during the progress of the reaction towards the equilibrium point and because the mass fraction of N_2 unanimously determines the fuel-to-air ratio. All other items were fitted as a function of these two variables.

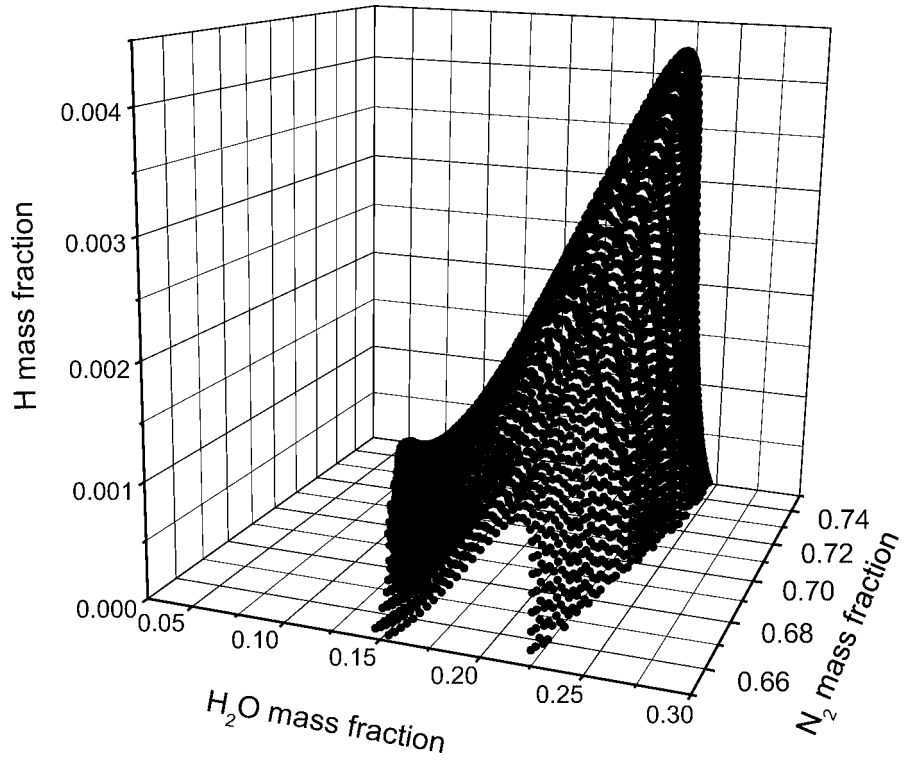

Figure 2. Points recorded in the repro-modelling database outline the 2D ILDM for hydrogen–air combustion.

Since the database is unstructured, the points were not evenly distributed. Using any fitting method, points that were close to each other had naturally higher weight in the fitting. This artefact was corrected by using a weight to each point during the fitting. This weight was inversely proportional to the density of other points near the actual point. Another problem is that the surface to be fitted is very steep in some regions and the fit would have a large error there. To compensate this effect, the original data points were transformed by multiplying their vectors by a rotating matrix. This transformation flattened the surface in the space of fitting variables. The transformed points were fitted and this approach solved the problem of steep gradients. Note that this transformation is similar to choosing other progress variables, which yield a better condition of the mapping.

Previously [15], multivariate adaptive splines using the MARS algorithm of Friedman [30] allowed very good fits for repro-modelling data. For the hydrogen combustion data the fit by the MARS method was not optimal, and a fitting method producing lower errors was desirable. Thus, we used the SURFIT program (NETLIB package, FITPACK collection), which is based on the spline fitting theory of Dierckx [31]. Further improvement was achieved by changing the original error control, which improved the quality of the fit considerably.

The fitted mechanism is available as a FORTRAN subroutine, which expects the actual values of the mass fractions of N_2 and H_2O as input and provides the corresponding mass fractions of all other species, temperature, production rate of water, and also the change of mass fraction of water after elapsed time Δt, where $\Delta t = 10^{-4}$ s and 10^{-5} s.

5. Testing the fitted mechanism

The fitted mechanism was tested against the full mechanism in homogeneous, constant pressure, adiabatic combustion simulations. Calculations with the detailed mechanism were done with program CONP of the CHEMKIN package [32], which uses the VODE stiff differential equation solver. In calculations with the repro-model, also the VODE integrator was used and the single variable of the differential equation was the water mass fraction. Integration provided the new value of water after an arbitrary time step, and then the fitted function was used to determine the concentrations of all other species.

Calculations were started from several hundred arbitrary initial compositions and usually good agreement was found with the detailed mechanism results. Figure 3 shows such a comparison. In this case agreement is good for all concentrations, except for slight deviations for radical OH. In general, agreement between the simulation results of the detailed and of the fitted mechanisms was poor for mixtures where the reaction had been started from near the cold boundary or near the burned state. At these conditions, however, the chemical reaction is quite slow, and the dynamics of a reacting flow (e.g., in flames) is controlled by mixing and diffusion. Therefore inaccurate predictions of the reaction rate do not induce high error to flame calculations.

In calculations with the fitted mechanism, temperature of the reaction mixture was calculated in two different ways. The fitted model provided temperature as a function of the actual N_2 and H_2O concentrations. An alternative method is to compute the temperature of the mixture from the composition of the gas and the enthalpy using the thermodynamic utility functions of CHEMKIN. Figure 3 shows that the temperatures calculated in these two ways are almost identical, which indicates that fitting of the temperature provides a good approximation and circumvents the computationally expensive calculation of it from enthalpy and gas composition.

Converting the original kinetic system of ODEs to a simplified system of differential equations has two effects: the number of variables decreases (here from 9 to 1) and also the stiffness of the ODE decreases. A practical measure of stiffness is the longest timestep that can be used for integration if an explicit ODE integrator, like the explicit Euler method, is used. In a series of calculations, the fitted model was integrated using a simple explicit Euler scheme and the time steps were systematically varied from $1 \cdot 10^{-8}$ s to $4 \cdot 10^{-6}$ s. These calculations represent a rough exploration only, but may indicate the tendencies properly. Figure 4 shows that for timesteps $1 \cdot 10^{-7}$ s and shorter, the solution was identical to the stiff ODE solver (VODE) solution and for longer timesteps there was a gradual deviation. Similar experiments were carried out with the detailed

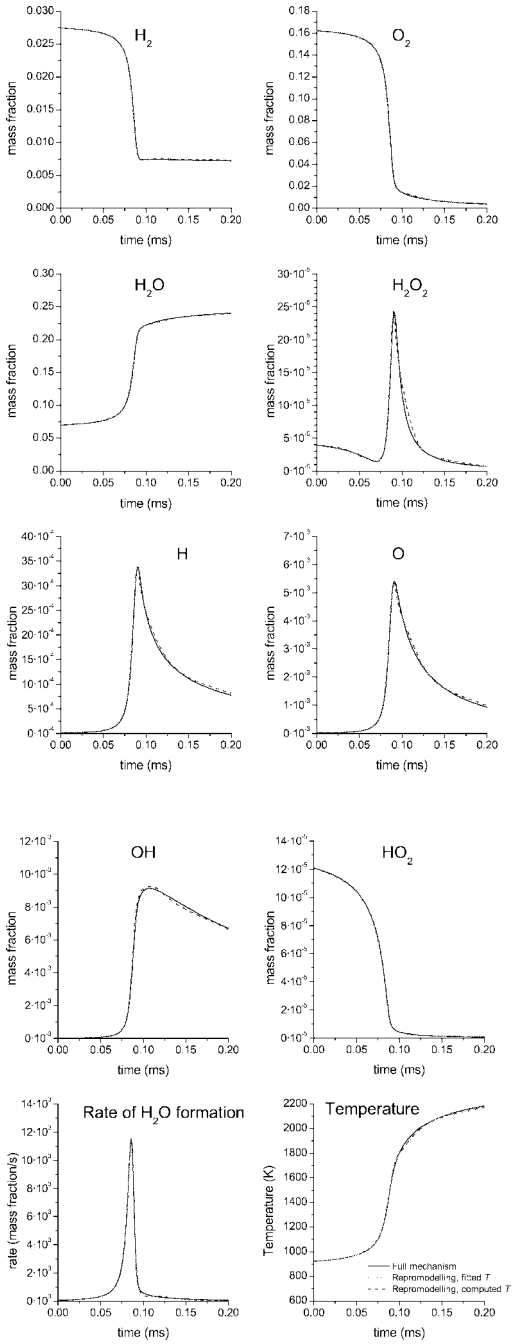

Figure 3. Spatially homogeneous, constant pressure, adiabatic combustion of hydrogen–air mixtures. Concentrations calculated using the detailed mechanism and the fitted model are denoted by solid and dashed lines, respectively. Temperature was calculated in three ways: using the detailed mechanism (solid line), the fitted temperature (dots), and from the (fixed) enthalpy and the fitted concentrations (dashes).

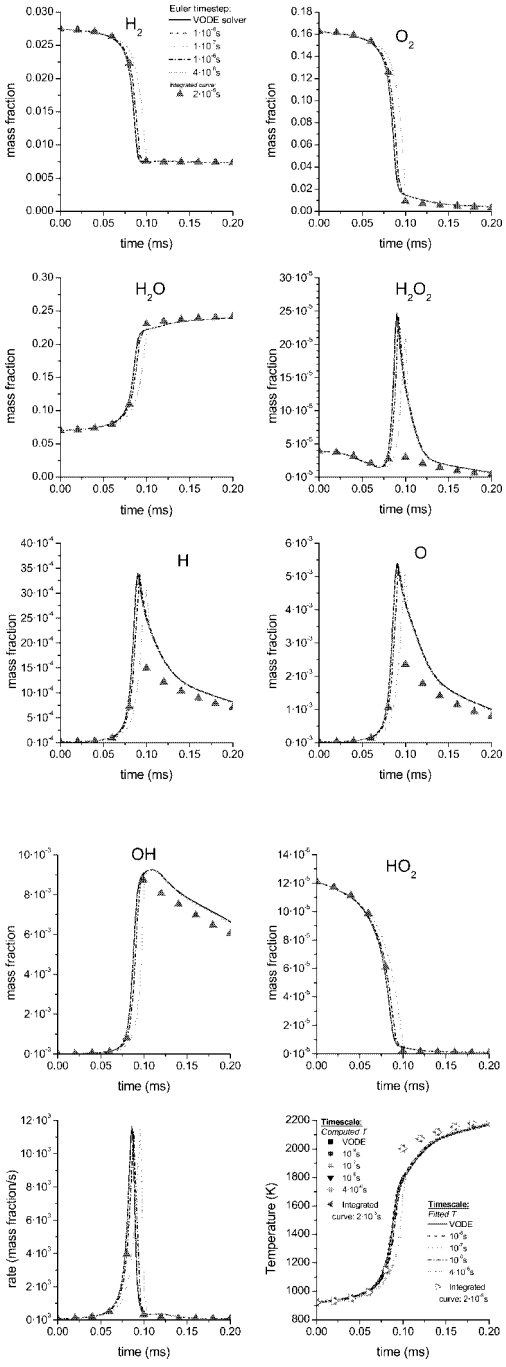

Figure 4. The fitted equations can be integrated even using a simple Euler equation, if the stepsize is less then 10^{-6} s.

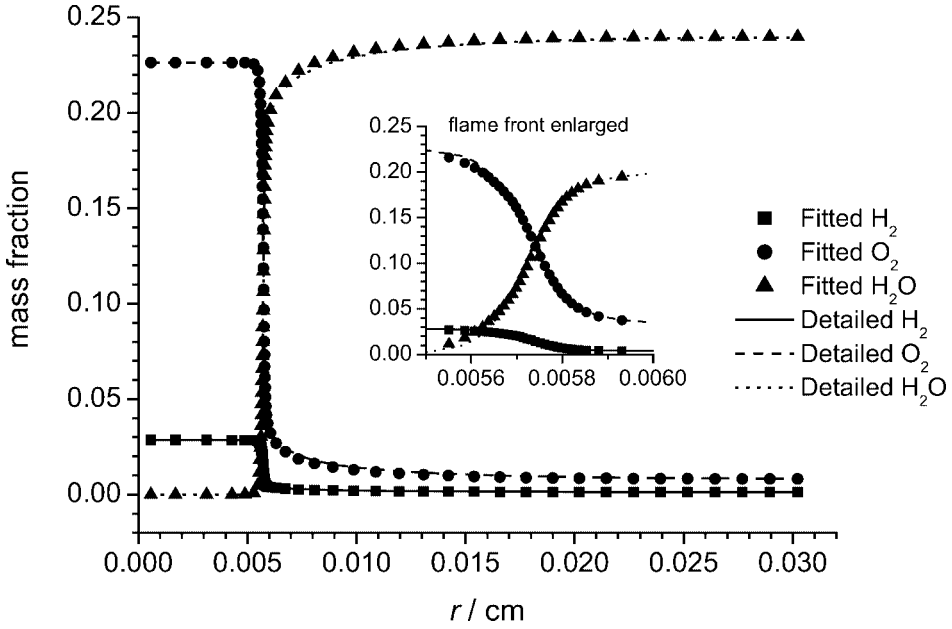

Figure 5. Simulation results for a stoichiometric, atmospheric premixed laminar hydrogen–air flat flame. Spatial profiles of the concentrations of major species calculated using the detailed mechanism (solid line) and the fitted model (dots).

mechanism and in this case timestep $1 \cdot 10^{-8}$ s gave good solution, while for all longer steps the calculation failed by causing number representation overflow. The reason is that changing from the original kinetic ODEs to the fitted model the stiffness decreased. The largest timestep that still provided accurate solution only slightly increased, but the solution was stable even at larger timesteps.

As described above, a fitted model was also created that predicted concentration changes during interval $\Delta t = 1 \cdot 10^{-5}$ s and $\Delta t = 1 \cdot 10^{-4}$ s. These fitted models proved to be accurate [33,34] compared to detailed chemical kinetic calculations in spite of using such relatively long time intervals.

As a second test, the fitted mechanism was used to simulate freely propagating laminar flat flames. For these calculations, the fitted model was implemented into code INSFLA [35], which was originally developed for the simulation of one-dimensional ignition processes and later extended to allow the simulation of one-dimensional laminar premixed flames and diffusion flames in counter flow configuration, using detailed and reduced reaction mechanisms [36]. Simulation results are compared in figures 5 and 6 for a stoichiometric, atmospheric hydrogen–air flat flame using the detailed mechanism and the fitted model. Figure 5 shows that there is a very good agreement everywhere for the concentrations of major species. Figure 6 indicates that in the postflame region there is some deviation for the concentration of radical OH, which can be attributed to the accuracy of the fit, while there is good agreement for radicals H and O. A closer look at the flame front shows that the agreement is good there even for radical OH.

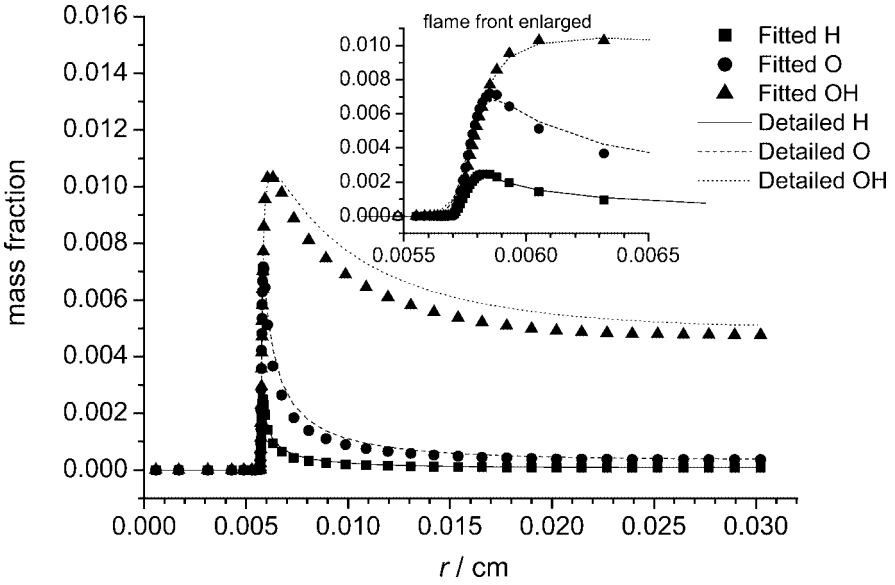

Figure 6. Simulation results for a stoichiometric, atmospheric premixed laminar hydrogen–air flat flame. Spatial profiles of the radical concentrations calculated using the detailed mechanism (solid line) and the fitted model (dots).

6. Conclusion

An algorithm is given for the repro-modelling based generation of intrinsic low-dimensional manifolds. It can be applied to any complex system having time scale separation and is based on monitoring the geometric dimension of the trajectory during the solution of ordinary differential equations that describe the system. If this dimension falls below a predefined limit, points of the trajectory are recorded in a database and fitted by multivariate functions. These functions can replace the original model in subsequent simulations. This algorithm represents a further development of the repro-modelling methodology and is at the same time an efficient method for the calculation of slow manifolds.

Using this method, a fitted model was created that described the combustion of hydrogen in air. The fitted model was tested in several homogeneous explosion simulations and laminar flame calculations and good agreement to the results obtained by using a detailed elementary mechanism was found. The fitted model has also been applied to the simulation of turbulent nonpremixed jet hydrogen–air flames using the PDF transport method [33,34].

Acknowledgements

Calculations and studies presented in this paper were backed by several sources, including OTKA grant No. T025875 from the Hungarian Science Foundation and grant

7UNPJ048687 from the Swiss National Science Foundation. Helpful discussions with A.S. Tomlin, H. Niemann and C. Frouzakis are welcome. The first version of the program for the generation of H_2/air manifold was elaborated during the visit of T. Turányi to the Heidelberg University.

References

[1] J. Warnatz, Resolution of gas phase and surface chemistry into elementary reactions, Proc. Combust. Inst. 24 (1992) 553–579.
[2] J. Warnatz, U. Maas and R.W. Dibble, *Combustion: Physical and Chemical Foundations, Experiments, Modeling and Simulation, Pollutant Formation, Applications* (Springer, Heidelberg, 1996).
[3] K.J. Hughes, T. Turányi, A.R. Clague and M.J. Pilling, Development and testing of a comprehensive chemical mechanism for the oxidation of methane, Int. J. Chem. Kinet. 33 (2001) 513–538.
[4] K.J. Hughes, A.S. Tomlin, E. Hampartsoumian, W. Nimmo, I.G. Zsély, M. Ujvári, T. Turányi, A.R. Clague and M.J. Pilling, An investigation of important gas phase reactions of nitrogen species from the simulation of bulk experimental data in combustion systems, Combust. Flame 124 (2001) 573–589.
[5] A.S. Tomlin, T. Turányi and M.J. Pilling, Mathematical tools for the construction, investigation and reduction of combustion mechanisms, in: *Low-Temperature Combustion and Autoignition*, ed. M.J. Pilling, Comprehensive Chemical Kinetics, Vol. 35 (Elsevier, Amsterdam, 1997), pp. 293–437.
[6] W.S. Meisel and D.C. Collins, Repro-modeling: An approach to efficient model utilization and interpretation, IEEE Trans. Systems, Man and Cybernetics 3/4 (1973) 349–358.
[7] A.M. Dunker, The reduction and parameterization of chemical mechanisms for inclusion in atmospheric reaction-transport models, Atmospheric Environ. 20 (1986) 479–486.
[8] C.M. Spivakovsky, S.C. Wofsy and M.J. Prather, A numerical method for parameterization of atmospheric chemistry: Computation of tropospheric OH, J. Geophys. Res. 95D (1990) 18433–18439.
[9] T. Turányi, Parameterization of reaction mechanisms using orthonormal polynomials, Comput. Chem. 18 (1994) 45–54.
[10] T. Turányi, Application of repro-modelling for the reduction of combustion mechanisms, Proc. Combust. Inst. 25 (1994) 948–955.
[11] A.R. Marsden, M. Frenklach and D.D. Reible, Increasing the computational feasibility of urban air quality models that employ complex chemical mechanisms, JAPCA 37 (1987) 370–376.
[12] R. Lowe and A.S. Tomlin, Low-dimensional manifolds and reduced chemical models for tropospheric chemistry simulations, Atmospheric Environ. 34 (2000) 2425–2436.
[13] R.M. Lowe, A.S. Tomlin, The application of repro-modelling to a tropospheric chemical model, Environ. Model. Software 15 (2000) 611–618.
[14] L.J. Clifford, A.M. Milne, T. Turányi and D. Boulton, An induction parameter model for shock-induced hydrogen combustion simulations, Combust. Flame 113 (1998) 106–118.
[15] A. Büki, T. Turányi, Gy. Solt and M. Braithwaite, Heat release in compressed bubbles containing alkane-air mixtures, manuscript in preparation.
[16] U. Maas and S.B. Pope, Simplifying chemical kinetics: Intrinsic low-dimensional manifolds in composition space, Combust. Flame 88 (1992) 239–264.
[17] O. Gicquel, D. Thévenin, M. Hilka and N. Darabiha, Direct numerical simulation of turbulent premixed flames using intrinsic low-dimensional manifolds, Combust. Theory Modelling 3 (1999) 479–502.
[18] U. Maas, Efficient calculation of intrinsic low-dimensional manifolds for the simplification of chemical kinetics, Comput. Vis. Sci. 1 (1998) 69–81.
[19] T. Blasenbrey, Entwicklung und Implementierung automatisch reduzierter Reaktionsmechanismen für die Verbrennung von Kohlenwasserstoffen, Ph.D. thesis, Stuttgart University (2000).

[20] U. Maas, Mathematical modeling of the coupling of chemical kinetics with flow and molecular transport, in: *Scientific Computing in Chemical Engineering*, eds. F. Keil, W. Mackens, H. Voss and J. Werther, Vol. II (Springer, 1999) pp. 26–56.
[21] U. Maas and D. Thévenin, Correlation analysis of direct numerical simulation data of turbulent nonpremixed flames, Proc. Combust. Inst. 27 (1998) 1183–1189.
[22] D. Schmidt and U. Maas, Analysis of the intrinsic low-dimensional manifolds of strained and unstrained flames, in: *Modelling of Chemical Reaction Systems, Proceedings of an International Workshop*, eds. J. Warnatz and F. Behrendt, Heidelberg, Germany, July 24–26 (1996).
[23] D. Schmidt, T. Blasenbrey and U. Maas, Intrinsic low-dimensional manifolds of strained and unstrained flames, Combust. Theory Modelling 2 (1998) 135–152.
[24] A.S. Tomlin, L. Whitehouse, R. Lowe and M.J. Pilling, Low dimensional manifolds in tropospheric chemical systems, Faraday Discussions 120 (2001) 125–146.
[25] S. Handrock-Meyer, L.V. Kalachev and K.R. Schneider, A method to determine the dimension of long-time dynamics in multi-scale systems, J. Math. Chem. 30 (2001) 133–160.
[26] Combustion simulations at the Leeds University and at the ELTE, available at http://www.chem.leeds.ac.uk/Combustion/Combustion.html or http://garfield.chem.elte.hu/Combustion/Combustion.html
[27] R.L.G.M. Eggels and L.P.H. de Goey, Mathematically reduced reaction mechanisms applied to adiabatic flat hydrogen–air flames, Combust. Flame 100 (1995) 559–570.
[28] U. Maas and S.B. Pope, Laminar flame calculations using simplified chemical kinetics based on intrinsic low-dimensional manifolds, Proc. Combust. Inst. 25 (1994) 1349–1356.
[29] S.B. Pope, Computationally efficient implementation of combustion chemistry using *in situ* adaptive tabulation, Combust. Theory Modelling 1 (1997) 41–63.
[30] J.H. Friedman, Multivariate adaptive regression splines, The Ann. Statist. 19 (1991) 1–141.
[31] P. Dierckx, *Curve and Surface Fitting with Spline Functions* (Oxford Univ. Press, Oxford, 1993).
[32] R.J. Kee, F.M. Rupley and J.A. Miller, CHEMKIN-II: A Fortran chemical kinetics package for the analysis of gas phase chemical kinetics, Sandia National Laboratory Report No. SAND89-8009B (1991).
[33] A. Obieglo, J. Gass, A. Büki and T. Turányi, PDF-Berechnung einer turbulenten Flamme unter Verwendung des Repromodellierens, VDI Berichte 1492 (1999) 487–492.
[34] A. Obieglo, J. Gass, A. Büki and T. Turányi, Simulation of a turbulent non-premixed H_2 flame using repro-modelling, Combust. Flame, submitted.
[35] U. Maas and J. Warnatz, Ignition processes in hydrogen–oxygen mixtures, Combust. Flame 74 (1988) 53–69.
[36] U. Maas, Coupling of chemical reaction with flow and molecular transport, Applications Math. 40 (1995) 249.